

# The prolate-to-oblate shape transition of phospholipid vesicles in response to frequency variation of an AC electric field can be explained by the dielectric anisotropy of a phospholipid bilayer

Primož Peterlin<sup>1</sup>, Saša Svetina<sup>1,2</sup>, and Boštjan Žekš<sup>1,2</sup>

<sup>1</sup>University of Ljubljana, Faculty of Medicine, Institute of Biophysics, Lipičeva 2, Ljubljana, Slovenia, <sup>2</sup>Jožef Stefan Institute, Jamova 39, Ljubljana, Slovenia

E-mail: primoz.peterlin@mf.uni-lj.si

**Abstract.** The external electric field deforms flaccid phospholipid vesicles into spheroidal bodies, with the rotational axis aligned with its direction. Deformation is frequency dependent: in the low frequency range ( $\sim 1$  kHz), the deformation is typically prolate, while increasing the frequency to the 10 kHz range changes the deformation to oblate. We attempt to explain this behaviour with a theoretical model, based on the minimization of the total free energy of the vesicle. The energy terms taken into account include the membrane bending energy and the energy of the electric field. The latter is calculated from the electric field via the Maxwell stress tensor, where the membrane is modelled as anisotropic lossy dielectric. Vesicle deformation in response to varying frequency is calculated numerically. Using a series expansion, we also derive a simplified expression for the deformation, which retains the frequency dependence of the exact expression and may provide a better substitute for the series expansion used by Winterhalter and Helfrich, which was found to be valid only in the limit of low frequencies. The model with the anisotropic membrane permittivity imposes two constraints on the values of material constants: tangential component of dielectric permittivity tensor of the phospholipid membrane must exceed its radial component by approximately a factor of 3; and the membrane conductivity has to be relatively high, approximately one tenth of the conductivity of the external aqueous medium.

PACS numbers: 87.16.Dg, 87.50.Rr, 77.84.-s, 41.20.Cv

Submitted to: *J. Phys.: Condens. Matter*

## 1. Introduction

Rapid development in biotechnology induced a growing interest in the influence of the AC electric field on biological cells, phospholipid vesicles and colloidal particles [1], which instigated theoretical investigations in this area [2, 3]. Among the systems studied,

phospholipid vesicles are often chosen as the model system of choice due to their well-defined structure.

In the late 1950s, Schwan [4] began a series of studies of the influence of the electric field on biological cells, modelling them as simple geometric shells with given electric properties. In the early 1970s, Helfrich included the then newly developed elastic theory for lipid bilayers [5] into the treatment of the effect of the external electric field on phospholipid vesicle shape [6]. The first experiments with phospholipid vesicles in an electric field which followed several years later [7] seemed to confirm the claim from the previous theoretical analysis [6]: a 2 kHz external AC electric field deforms flaccid phospholipid vesicles into *prolate* spheroids. Winterhalter and Helfrich [8] extended the earlier theoretical treatment [6]; their model allows for a finite electrical resistance of the bilayer, an AC electric field, and includes Maxwell stresses inside the membrane. The authors treated the spherical vesicle as a lossy dielectric immersed into a medium which was also treated as a lossy dielectric. They examined the case  $\sigma_m/\sigma_w \ll \epsilon_m/\epsilon_w$ , where  $\sigma_m$ ,  $\sigma_w$ ,  $\epsilon_m$  and  $\epsilon_w$  are the conductivities and permittivities of the membrane and the aqueous medium, respectively. Employing series expansions, they obtained a simple expression for vesicle deformation and predicted a conducting regime of vesicle behaviour at low frequencies ( $\omega \ll \sigma_m/\epsilon_m$ ), where the field does not penetrate the vesicle interior, a dielectric regime at higher frequencies ( $\omega \gg \sigma_w/\epsilon_w$ ), where the field penetrates the vesicle interior, and an intermediate regime in between the two. In all three regimes, they obtained a prolate vesicle shape.

In contrast to that, experiments with varying frequency [9, 10] have demonstrated that a vesicle undergoes a *prolate-to-oblate shape change* when the frequency of the applied field is increased from the 1 kHz range into the 10-kHz range (figure 1a). Figure 1b shows the dependence of the ratio of vesicle semiaxes  $c/a$  for the shown vesicle on the frequency of the applied electric field, with  $c$  being the semiaxis parallel to the field, and  $a$  the semiaxis perpendicular to it.

In this paper, we take the work of Winterhalter and Helfrich as our starting point and proceed to extend it by allowing for an anisotropy of the permittivity of the phospholipid bilayer. Since the model of Winterhalter and Helfrich departs from the experimental data in the high-frequency region by failing to predict oblate shapes, we sought a modification that would affect its behaviour in the high-frequency range, where the behaviour of the system is governed solely by the permittivities.

Recently, several papers have been published which take into account the anisotropy of the membrane dielectric permittivity and the membrane electric conductivity, which arise due to adsorbed hydrophobic ions on the membrane [11, 12]. Ambjörnsson and Mukhopadhyay [13] have provided a solution for the electric potential for a general ellipsoid coated with a dielectrically anisotropic coating; the same group also examined a possible mechanism for the dielectric anisotropy in the membrane at frequencies where molecular resonances are important [14]. Simeonova and Gimsa [15] have extended the description of the phospholipid vesicle membrane to a three-layer shell to take into account the fact that the dielectric anisotropy occurs only in the phospholipid headgroup

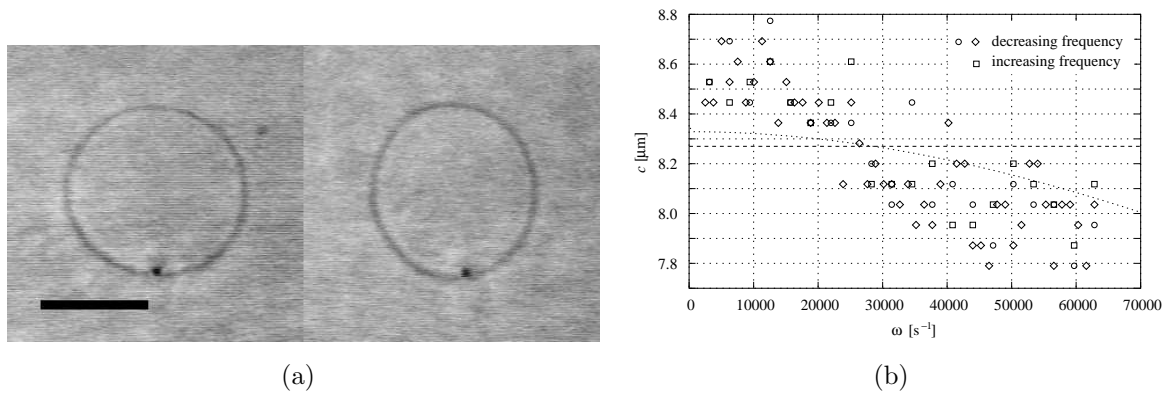


**Figure 1.** (a) Giant phospholipid vesicle is deformed into a prolate shape (left) at an applied AC field of 1 kHz, and into an oblate shape at 10 kHz (right). The conductivity of the aqueous medium was  $1.3 \mu\text{S}/\text{cm}$ . An electric field of  $\approx 2 \cdot 10^4 \text{ V}/\text{m}$  was applied in the horizontal direction. The bar represents  $10 \mu\text{m}$ . (b) Deformation of the same vesicle, expressed as the value of the semiaxis  $c$  (aligned with the direction of the electric field) as a function of the circular frequency  $\omega$  of the external AC electric field. The dashed line corresponds to the value at which the vesicle is spherical; greater values of  $c$  correspond to prolate shapes, smaller to oblate. The dotted line is discussed further in the text. The three consecutive runs yield  $2394 \pm 75$ ,  $2427 \pm 75$  and  $2371 \pm 87 \mu\text{m}^3$ , as estimates for the vesicle volume, respectively, which indicates that the vesicle volume did not change significantly during the experiment. Details on experimental setup are given in [20].

layer, while the middle layer of hydrocarbon chains is mainly isotropic. It also needs to be noted that transitions between prolate and oblate shapes in response to a frequency variation of the applied electric field have been examined theoretically for cases where the electrical properties of the aqueous solution inside the vesicle differ from those in the vesicle exterior [16, 17], and recently, an experimental morphological phase diagram has also been obtained [18]. A review of the studies of the influence of the electric field on phospholipid vesicles was recently summarized in a paper by Dimova and coworkers [19].

While the above papers provide an analytical expression for the electric potential [13] or a thorough numerical analysis of the Clausius-Mossotti factor [11, 12, 15], they do not focus on an analysis of parameters at which either prolate or oblate deformation is possible in the high- and low-frequency limit, which is the aim of this paper.

The paper is organized as follows. In section 2 we first develop an extension of the model of Winterhalter and Helfrich by taking into account the anisotropy of membrane permittivity. In section 3 we show that the model presented here exhibits frequency-dependent prolate-to-oblate shape transition of a phospholipid vesicle similar to the one observed in the experiment. In the expansion valid for large vesicles, we derive the necessary conditions for a prolate or oblate deformation in both the high- and low-frequency limit, and analyse the dependence of the prolate-to-oblate shape transition frequency on material constants. Finally, in section 4, we discuss some of the issues

which arise from the results.

## 2. Theoretical framework

The equilibrium vesicle shape in an external electric field is calculated as the shape with the minimal total free energy, consisting of the vesicle bending energy and the energy due to the electric field. The calculation was conducted for a vesicle with constant volume, while the necessary area increase for the deformation stems from the flattening of thermal fluctuations of the vesicle by the electric field [21, 22]. The analytical expression for the membrane bending energy is well known [5], and the change of the energy due to the electric field is calculated as the work done by the force of the electric field while deforming the vesicle [8]. In order to evaluate it, we first have to calculate the electric field. The present treatment is limited to small deviations of vesicle shape from the sphere, thus the electric field in the presence of a spherical shell is computed. Both the aqueous solution inside and outside the vesicle and the vesicle membrane are treated as lossy dielectrics. The aqueous solutions inside and outside the vesicle have identical electrical properties. Dielectric permittivity of the membrane is treated as anisotropic, with the component aligned with the normal to the membrane differing from the components perpendicular to this direction. Both the dielectric permittivity and the electric conductivity of the aqueous solution as well as the electric conductivity of the membrane are treated as scalars.

The applied electric field  $\mathbf{E}$  introduces a single distinct axis into the system, so the treatment can be limited to axially symmetric shapes. This eliminates the dependence on the longitude angle  $\phi$ , if the polar ( $z$ ) axis is chosen parallel to the applied field. Thus, the vesicle surface can be parametrized as

$$r(\theta) = s_0 + s(\theta) , \quad (1)$$

where  $|s(\theta)| \ll s_0$ ,  $s_0$  denoting the deformation independent of the polar angle  $\theta$ . In an absence of deformation ( $|s(\theta)| = 0$ ),  $s_0$  equals the radius of the undeformed sphere  $r_0$ . The deformation is independent of the sign of the electric field, thus it is proportional to  $E^2$  in the lowest order. As the field itself is proportional to  $\cos \theta$ , one can expect a deformation coupled with a field to be proportional to  $\cos^2 \theta$ . In terms of expansion into spherical harmonics, this limits us to a sum of even terms. Retaining only the terms proportional to  $E^2$  or lower, a quadrupolar term remains, where  $s(\theta)$  equals the second Legendre polynomial:  $s(\theta) = \frac{1}{2}s_2(3 \cos^2 \theta - 1)$ , with  $s_2$  being a measure for the extent of deformation. Positive values of  $s_2$  indicate prolate deformation, negative oblate.

If the membrane area is to be locally conserved, a quadrupolar displacement  $\delta r_r$  in a radial direction must be accompanied by a tangential displacement  $\delta r_\theta$  [8]:

$$\delta r_r = \frac{1}{2}(3 \cos^2 \theta - 1) s_2 \quad (2a)$$

$$\delta r_\theta = -\cos \theta \sin \theta s_2 . \quad (2b)$$

A requirement for a local area conservation assures that the membrane stretching is independent of polar angle  $\theta$ . The total membrane area expansion is determined by

the relationship between  $s_0$  and  $r_0$ . Taking into account the requirement for a constant vesicle volume, the following relationship for  $s_0$  is obtained:

$$s_0 = r_0 - \frac{s_2^2}{5r_0}. \quad (3)$$

The correction for a constant volume (3) contains a higher term in the powers of  $s_2$  and thus does not affect in the lowest term either the bending energy or the energy due to the electric field, yielding  $s_0 = r_0$  an adequate approximation.

For small deformations, quadrupolar deformation only induces small perturbative changes in the vesicle bending energy and the energy due to the electric field.

$$G_{\text{bend}}(s_2) \approx G_{\text{bend}}(s_2 = 0) + \frac{1}{2} \left. \frac{\partial^2 G_{\text{bend}}}{\partial s_2^2} \right|_{s_2=0} s_2^2 \quad (4)$$

$$G_{\text{field}}(s_2) \approx G_{\text{field}}(s_2 = 0) + \left. \frac{\partial G_{\text{field}}}{\partial s_2} \right|_{s_2=0} s_2 \quad (5)$$

The total energy of the vesicle formally depends on two parameters,  $r_0$  and  $s_2$ . The constraint requiring a constant vesicle volume however eliminates one degree of freedom, yielding (4–5). It is also worth noting that the fact that neither prolate ( $s_2 > 0$ ) nor oblate shapes ( $s_2 < 0$ ) have a bending energy lower than those of a sphere means that the expansion for the bending energy (4) contains no linear term.

Equilibrium vesicle deformation, expressed in terms of  $s_2$ , can then be calculated by minimizing the total free energy over  $s_2$ :

$$\frac{d}{ds_2} (G_{\text{bend}} + G_{\text{field}}) = \left. \frac{\partial^2 G_{\text{bend}}}{\partial s_2^2} \right|_{s_2=0} s_2 + \left. \frac{\partial G_{\text{field}}}{\partial s_2} \right|_{s_2=0} = 0. \quad (6)$$

Equation (6) gives the extent of deformation ( $s_2$ ) at given conditions.

It is now our task to write an expression for the vesicle bending energy (4), which can be written as [5]:

$$G_{\text{bend}} = \frac{1}{2} k_c \oint (c_1 + c_2)^2 dA. \quad (7)$$

Here,  $k_c$  is the bending elastic modulus of the membrane, while  $c_1$  and  $c_2$  are the principal curvatures of the membrane. The spontaneous curvature  $c_0$  has been omitted, because it vanishes for a bilayer composed of two equal layers. The integration is conducted over the total membrane area  $A$  of a quadrupolarly deformed vesicle. Up to quadratic order terms in  $s_2$ , the total bending energy of a nearly spherical vesicle can be written as [5]:

$$G_{\text{bend}} = 8\pi k_c + \frac{48\pi}{5} k_c \left( \frac{s_2}{r_0} \right)^2. \quad (8)$$

This can be readily interpreted as the bending energy of a sphere plus an addition due to the quadrupolar deformation.

The free energy term arising from the electric field (5) is calculated as the work done by the forces of the electric field during the deformation of the vesicle. In order to evaluate it, we first have to calculate the electric field around a vesicle (figure 2). Gauss' law  $\nabla \cdot \mathbf{D} = 0$  together with the requirement for an irrotational electric field

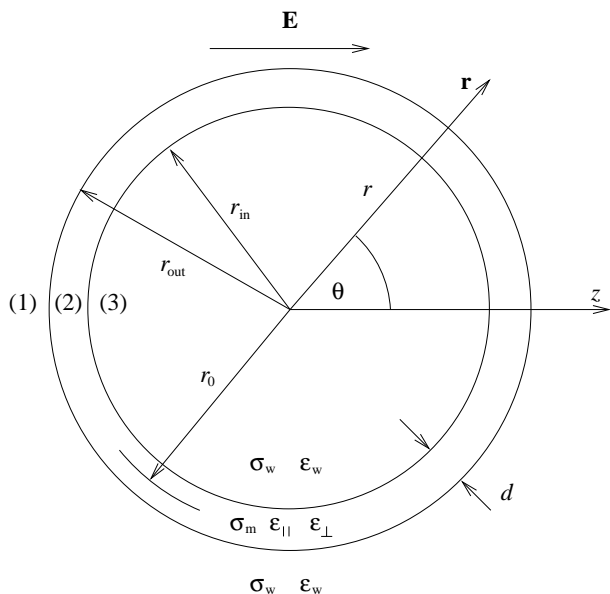


**Figure 2.** A vesicle is modelled in spherical coordinates  $(r, \theta)$  as a spherical shell with the external radius  $r_{\text{out}} = r_0 + d/2$  and the internal radius  $r_{\text{in}} = r_0 - d/2$  ( $d \ll r_{\text{in}}$  being the membrane thickness) exposed to an external electric field  $\mathbf{E}$ . The conductivity and permittivity of the aqueous solution inside and outside the membrane are denoted by  $\sigma_w$  and  $\epsilon_w$ , and the membrane conductivity is denoted by  $\sigma_m$ . Membrane permittivity is in general anisotropic, hence  $\epsilon_{\parallel}$ ,  $\epsilon_{\perp}$ ; their orientation is defined in the text (equation 11). The three media, vesicle exterior, vesicle membrane and vesicle interior are denoted by (1), (2), and (3), respectively.

$\nabla \times \mathbf{E} = 0$ , which stems from Faraday's law for electromagnetic induction, yields the Laplace equation for the electric potential  $U$  in a medium with homogenous dielectric permittivity [23] – in our case the aqueous medium in the vesicle interior and the external aqueous medium (respectively denoted by (3) and (1) in figure 2). In the anisotropic case, however, Gauss' law does not lead to the Laplace equation for the electric potential  $U$ ,  $\nabla \cdot \mathbf{D} = \nabla \cdot \underline{\epsilon} \mathbf{E} = -\nabla \cdot (\underline{\epsilon} \nabla U)$ . Here,  $\mathbf{D}$  is the displacement field,  $\mathbf{E}$  is the electric field and  $\underline{\epsilon}$  is the permittivity tensor.

The boundary conditions on both the outer and the inner membrane-water boundary impose  $\nabla \times \mathbf{E} = 0$ , thus requiring the continuity of the tangential component of the electric field, and that the total surface charge density, including both free charge and displacement charge, must vanish. In the spherical geometry, this yields the equations

$$E_{\theta}^{(1)} = E_{\theta}^{(2)}, \quad (9)$$

$$(\epsilon_w - i\omega\sigma_w)E_r^{(1)} = (\epsilon_{\parallel} - i\omega\sigma_m)E_r^{(2)}, \quad (10)$$

for the (1–2) interface ( $r = r_{\text{out}}$ , figure 2) and similarly for the (2–3) interface ( $r = r_{\text{in}}$ ). Apart from (9–10), the system is constrained by two additional conditions: one requiring that the electric field far from the vesicle is unperturbed, and the other requiring that the electric field is finite inside the vesicle.

In (9,10) we introduced the notation for the dielectric permittivities and electric conductivities in the three media:  $\epsilon^{(1)} = \epsilon^{(3)} = \epsilon_w$ ,  $\sigma^{(1)} = \sigma^{(3)} = \sigma_w$ , and  $\sigma^{(2)} = \sigma_m$ . The

membrane permittivity is treated as anisotropic. Due to its structure, electric properties in the direction along the long axis of phospholipid molecules (or normal to the vesicle membrane) are expected to be markedly different from the properties in the direction perpendicular to it. The phospholipid molecule is not axially symmetric per se, but due to the unordered liquid-like structure of the bilayer we can approximate it as such on the timescale of interest to our problem. The two directions perpendicular to the normal on the membrane can thus be treated as being equal. The component along the normal to the membrane is denoted by  $\epsilon_{\parallel}$  and the permittivity in the direction perpendicular to it by  $\epsilon_{\perp}$ . Local permittivity in a given point on the membrane is thus equal to  $\epsilon_{\parallel}$  in the normal direction and  $\epsilon_{\perp}$  in the tangential direction. Permittivity tensor is locally defined as:

$$\underline{\epsilon} = \begin{bmatrix} \epsilon_{\parallel} & 0 & 0 \\ 0 & \epsilon_{\perp} & 0 \\ 0 & 0 & \epsilon_{\perp} \end{bmatrix}. \quad (11)$$

For a spherical shell, local coordinates conveniently coincide with the spherical coordinates. Gauss' law  $\nabla \cdot (\underline{\epsilon} \nabla U) = 0$  for the treated geometry is most conveniently written in spherical coordinates,

$$\epsilon_{\parallel} \frac{1}{r^2} \frac{\partial}{\partial r} \left( r^2 \frac{\partial U}{\partial r} \right) + \epsilon_{\perp} \frac{1}{r^2 \sin \theta} \frac{\partial}{\partial \theta} \left( \sin \theta \frac{\partial U}{\partial \theta} \right) = 0. \quad (12)$$

In spherical coordinates, the equation can be separated into the radial and the angular parts,  $U(r, \theta) = R(r)\Theta(\theta)$  (it has been already taken into account that the problem is axially symmetrical and thus independent of  $\phi$ ), yielding two separate equations for the radial and the angular part. For the angular part, a Legendre differential equation is obtained. The equation obtained for the radial part differs from the spherical Bessel equation by involving a factor  $\epsilon_{\perp}/\epsilon_{\parallel}$  in the second term:

$$\frac{1}{r^2} \frac{d}{dr} \left( r^2 \frac{dR}{dr} \right) - \frac{\epsilon_{\perp}}{\epsilon_{\parallel}} \frac{l(l+1)}{r^2} R = 0. \quad (13)$$

It is worth noting that (13) represents a special case of Heun's equation, which arises from solving the case of a general ellipsoid [13]. Equation (13) is solved by a linear combination

$$R_l(r) = C_1 r^{\frac{1}{2}(-1 - \sqrt{1 + 4l\epsilon_{\perp}/\epsilon_{\parallel} + 4l^2\epsilon_{\perp}/\epsilon_{\parallel}})} + C_2 r^{\frac{1}{2}(-1 + \sqrt{1 + 4l\epsilon_{\perp}/\epsilon_{\parallel} + 4l^2\epsilon_{\perp}/\epsilon_{\parallel}})}.$$

The symmetry requirements of our problem limit us to the case  $l = 1$ . Thus, the ansatz for the electric potential that satisfies Gauss' law for the anisotropic case is

$$U^{(2)} = \frac{1}{2} \left[ \left( a^{(2)} r^{(\alpha-1)/2} + b^{(2)} r^{(-\alpha-1)/2} \right) \cos \theta e^{-i\omega t} + \text{C.C.} \right]. \quad (14)$$

A shorthand notation  $\alpha = \sqrt{1 + 8\epsilon_{\perp}/\epsilon_{\parallel}}$  has been introduced along the way. The isotropic case corresponds to  $\alpha = 3$ , which simplifies (14) to a known form

$$U^{(k)} = \frac{1}{2} \left[ \left( a^{(k)} r + \frac{b^{(k)}}{r^2} \right) \cos \theta e^{-i\omega t} + \text{C.C.} \right], \quad k = 1, 3. \quad (15)$$

The coefficients  $a^{(k)}$ ,  $b^{(k)}$ ;  $k = 1, 2, 3$ , can in general be complex to allow for a phase shift, and are determined from the boundary conditions.

The boundary conditions for the unperturbed field far away from the vesicle and the finite field inside the vesicle immediately yield two coefficients:

$$a^{(1)} = -E_0 \quad (16)$$

$$b^{(3)} = 0 \quad (17)$$

The remaining four coefficients are determined by the four equations specifying boundary conditions (9, 10):

$$a^{(2)} = \frac{-6E_0 r_{\text{out}}^{(3-\alpha)/2} (2 + \beta + \alpha\beta)}{8 + (2 + 6\alpha)\beta + (\alpha^2 - 1)\beta^2 - [8 + (2 - 6\alpha)\beta + (\alpha^2 - 1)\beta^2] \gamma^\alpha} \quad (18a)$$

$$a^{(3)} = \frac{-12E_0 \alpha \beta \gamma^{(\alpha-3)/2}}{8 + (2 + 6\alpha)\beta + (\alpha^2 - 1)\beta^2 - [8 + (2 - 6\alpha)\beta + (\alpha^2 - 1)\beta^2] \gamma^\alpha} \quad (18b)$$

$$b^{(1)} = \frac{E_0 r_{\text{out}}^3 [(\alpha - 1)\beta - 2] (2 + \beta + \alpha\beta) (1 - \gamma^\alpha)}{8 + (2 + 6\alpha)\beta + (\alpha^2 - 1)\beta^2 - [8 + (2 - 6\alpha)\beta + (\alpha^2 - 1)\beta^2] \gamma^\alpha} \quad (18c)$$

$$b^{(2)} = \frac{-6E_0 r_{\text{out}}^{(3+\alpha)/2} [(\alpha - 1)\beta - 2] \gamma^\alpha}{8 + (2 + 6\alpha)\beta + (\alpha^2 - 1)\beta^2 - [8 + (2 - 6\alpha)\beta + (\alpha^2 - 1)\beta^2] \gamma^\alpha} \quad (18d)$$

Consistently with [8], two more shorthand notations have been introduced:

$$\beta = \frac{\sigma_m - i\omega\epsilon_{\parallel}}{\sigma_w - i\omega\epsilon_w}, \quad (19)$$

$$\gamma = \frac{r_{\text{in}}}{r_{\text{out}}}. \quad (20)$$

The surface density of the force exerted on the boundary of dielectrics by the electric field is equal to the scalar product of the Maxwell stress tensor and the normal vector to the membrane,

$$\mathbf{f}_{\text{out}} = (\underline{T}^{(1)} - \underline{T}^{(2)}) \mathbf{e}_r, \quad (21a)$$

$$\mathbf{f}_{\text{in}} = (\underline{T}^{(2)} - \underline{T}^{(3)}) \mathbf{e}_r. \quad (21b)$$

The force vanishes in a homogeneous medium, but can in general be non-zero on the boundaries of media with different electrical properties. The Maxwell stress tensor is defined as

$$\underline{T} = \mathbf{D} \otimes \mathbf{E} - \frac{1}{2} (\mathbf{D} \cdot \mathbf{E}) \underline{I}, \quad (22)$$

where  $\underline{I}$  denotes the identity matrix.

Unlike in the case of the bending energy term in the total free energy (8), for which an analytical expression was obtained, an approach where energy difference is computed is employed here.  $\delta G_{\text{field}}$  denotes a small change in the energy due to the electric field, when a sphere ( $s_2 = 0$ ) is perturbed by a small deformation change  $\delta s_2$ . This energy difference is calculated as the work done by the forces of electric field during the displacement of membrane elements  $\delta \mathbf{r}$  (equations 2a,2b), integrated over the entire membrane area [8]:

$$\delta G_{\text{field}} = - \oint (\mathbf{f}_{\text{out}} \cdot \delta \mathbf{r}) dA_{\text{out}} - \oint (\mathbf{f}_{\text{in}} \cdot \delta \mathbf{r}) dA_{\text{in}}. \quad (23)$$



The integration is conducted over a sphere, which is consistent with the limit of small deformations ( $s_2 \ll r_0$ ).

Substituting the coefficients (18a–18d) into (23) yields a lengthy expression for  $\delta G_{\text{field}}$ , which will not be reproduced here. After substituting the expression (19) for  $\beta$  into it, one obtains an expression of the form  $(A + B\omega^2 + C\omega^4)/(D + E\omega^2 + F\omega^4)$ , which can be written as a sum of two dispersion terms:

$$\frac{dG_{\text{field}}}{ds_2} \rightarrow \frac{\delta G_{\text{field}}}{s_2} = -\frac{6\pi}{5} E_0^2 \epsilon_w r_{\text{out}}^2 \left( \xi_\infty + \frac{\xi_1}{1 + \omega^2 \tau_1^2} + \frac{\xi_2}{1 + \omega^2 \tau_2^2} \right), \quad (24)$$

where the coefficients  $\xi_\infty$ ,  $\xi_1$ ,  $\xi_2$ ,  $\tau_1$  and  $\tau_2$  are rather lengthy expressions involving five different material constants:  $\epsilon_{\parallel}$ ,  $\epsilon_{\perp}$ ,  $\epsilon_w$ ,  $\sigma_m$ ,  $\sigma_w$ , the membrane thickness  $d$  and the vesicle radius  $r_0$ . It turns out, however, that the actual number of independent parameters is lower. By introducing a dimensionless frequency  $\omega/(\sigma_w/\epsilon_w)$ , one can reduce the frequency dependence of (24) to only four parameters. Here, we have chosen them to be  $\gamma$ ,  $\epsilon_{\parallel}/\epsilon_w$ ,  $\Delta\epsilon/\epsilon_w$  and  $\sigma_m/\sigma_w$ .

Equilibrium vesicle deformation can finally be calculated by minimizing the total free energy (6) over  $s_2$ , yielding

$$s_2 = \frac{1}{16} \frac{r_0^4 \epsilon_w E_0^2}{k_c} \left( \xi_\infty + \frac{\xi_1}{1 + \omega^2 \tau_1^2} + \frac{\xi_2}{1 + \omega^2 \tau_2^2} \right), \quad (25)$$

where  $r_0^2 r_{\text{out}}^2$  has been replaced by  $r_0^4$ , consistent with the expansion in  $E^2$  and retaining the terms with the lowest energy. As we can see, the dependence of vesicle deformation  $s_2$  on the circular frequency  $\omega = 2\pi\nu$  contains two dispersion terms of the Maxwell-Wagner type, which arise due to the interfacial polarization and not due to intrinsic dispersion. It is also worth emphasizing that the only approximation used in deriving the expression (25) is that of a small deformation ( $s_2 \ll r_0$ ).

The coefficients  $\xi_\infty$ ,  $\xi_1$ ,  $\xi_2$ ,  $\tau_1$  and  $\tau_2$  figuring in (25) can be simplified using expansion in  $(1 - \gamma)$ , as  $(1 - \gamma) \lesssim 10^{-3}$  (the vesicle radius is in the range 1–100  $\mu\text{m}$ , while the thickness of the phospholipid membrane is approximately 4 nm). Expansion up to the first order in  $(1 - \gamma)$  yields:

$$\xi_\infty = -\frac{2[-2\epsilon_{\parallel}(\epsilon_w - \epsilon_{\parallel})^2 + (\epsilon_w + 2\epsilon_{\parallel})\epsilon_w\Delta\epsilon + 2\epsilon_{\parallel}(\Delta\epsilon)^2]}{9\epsilon_{\parallel}^2\epsilon_w} (1 - \gamma), \quad (26)$$

$$\xi_1 = \frac{-4\epsilon_{\parallel}\sigma_m\sigma_w(\epsilon_w - \epsilon_{\parallel}) + 2\sigma_w(\epsilon_{\parallel}\sigma_w + \epsilon_w\sigma_m + 2\epsilon_{\parallel}\sigma_m)\Delta\epsilon}{9\epsilon_{\parallel}^2\sigma_m^2} \left( \frac{\sigma_m}{\sigma_w} - \frac{\epsilon_{\parallel}}{\epsilon_w} \right) (1 - \gamma), \quad (27)$$

$$\xi_2 = \frac{8(\epsilon_{\parallel} + \Delta\epsilon)}{9\epsilon_{\parallel}} \left( \frac{\sigma_m}{\sigma_w} - \frac{\epsilon_{\parallel}}{\epsilon_w} \right) (1 - \gamma), \quad (28)$$

$$\tau_1 = \frac{\epsilon_{\parallel}}{\sigma_m}, \quad (29)$$

$$\tau_2 = \frac{\epsilon_w}{\sigma_w}. \quad (30)$$

We have introduced dielectric anisotropy  $\Delta\epsilon = \epsilon_{\perp} - \epsilon_{\parallel}$ . The characteristic times  $\tau_1$  and  $\tau_2$  correspond to the trans-membrane and the trans-vesicle-interior relaxations, respectively. It is worth noting that neither  $\tau_1$  nor  $\tau_2$  is affected by the anisotropy in this first-order approximation.

### 3. Results

This section consists of four points. First, we plot the dependence of deformation on frequency and comment on the effects of different material constants. Next, we look for the conditions where an oblate deformation ( $s_2 < 0$ ) exists in the high-frequency limit. A similar search is performed for the conditions where a prolate deformation ( $s_2 > 0$ ) exists in the low-frequency limit. Finally, we plot and analyse the dependence of the prolate-to-oblate transition frequency on material constants.

*Dependence of deformation on frequency.* Figure 3 shows the vesicle deformation as a function of the circular frequency  $\omega$  of the applied external electric field. Even though the expression for deformation (25) contains two dispersion terms, only one of them is prominent on the diagram. This is because at values of the parameters used for evaluation ( $\epsilon_{\parallel} \ll \epsilon_w$ ,  $\sigma_m \ll \sigma_w$ ), the magnitude of the second dispersion term is about two orders of magnitude smaller,  $\xi_2 \ll \xi_1$ . This agrees with the expressions (27,28) where expansion in  $(1 - \gamma)$  is used:  $\xi_2 \propto \sigma_m/\sigma_w$ , while  $\xi_1 \propto (\epsilon_w/\epsilon_{\parallel})(\sigma_w/\sigma_m)$ .

Figure 1b provides a comparison of the results of the model with experimental data. The parameters used to calculate the dotted line in figure 1b were  $k_c = 0.9 \times 10^{-19}$  J,  $E_0 = 200$  V/cm,  $\sigma_w = 10^{-4} \Omega^{-1}\text{m}^{-1}$ ,  $\sigma_m = 0.38 \times 10^{-5} \Omega^{-1}\text{m}^{-1}$ ,  $\epsilon_w = 80\epsilon_0$ ,  $\epsilon_{\parallel} = 2\epsilon_0$ ,  $\Delta\epsilon = 5.2\epsilon_0$ . While the results of the model reproduce a general trend, it is clear that its agreement with the experimental data is only qualitative. This can be attributed to the perturbative nature of the model, which is only valid for small deviations from a sphere only. This limitation is somewhat conflicting with the experimental requirements, where significant deviations from a sphere are clearly preferred for giving a more accurate readout.

The frequency-dependent prolate-to-oblate transition does not reflect a change of sign in the forces of the electric field – both in the high- and the low-frequency limit, the forces induced by the electric field pull the vesicle apart at poles and compress it around the equator, thus favouring a prolate deformation. A lower energy for an oblate shape at high frequencies stems from the shear term,  $f_{\theta} \delta r_{\theta}$ . In the high-frequency limit,  $f_{\theta}$  is zero for the isotropic case, and increases in magnitude with the increasing anisotropy  $\Delta\epsilon$ .

*High-frequency limit.* High-frequency behaviour depends only on the dielectric permittivities of the membrane and the aqueous solution, and is completely determined by coefficient  $\xi_{\infty}$  as can be seen from (25): if  $\xi_{\infty} > 0$ , the deformation is prolate, and vice versa. The sign of the exact expression for the coefficient  $\xi_{\infty}$  (without employing an expansion in  $(1 - \gamma)$ ) depends on two parameters; here, they were chosen to be  $\epsilon_{\parallel}/\epsilon_w$  and  $\Delta\epsilon/\epsilon_w$ . It is worth noting that while the expression  $\xi_{\infty}$  depends on  $\gamma$  as well, varying  $\gamma$  can not change its sign. Furthermore, for all values of vesicle radius which are of experimental interest,  $\gamma \approx 1$  holds, so  $\gamma$  does not significantly affect vesicle behaviour in our model, therefore we did not put much emphasis on it. Values of  $\epsilon_{\parallel}/\epsilon_w$  and  $\Delta\epsilon/\epsilon_w$

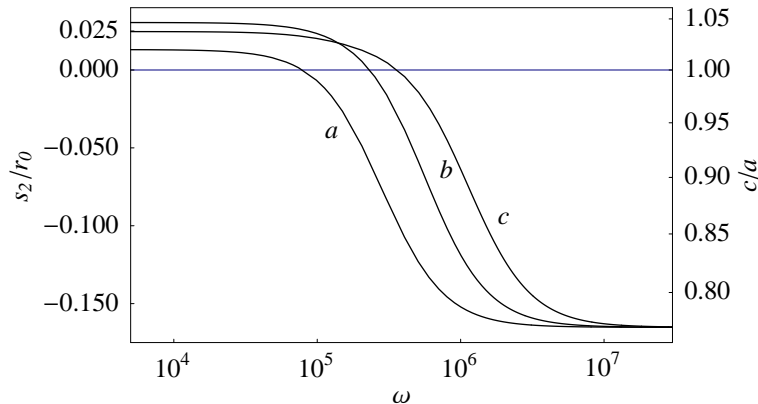


**Figure 3.** The theoretical dependence of vesicle deformation, expressed as either  $s_2/r_0$  (left axis) or  $c/a$  (right axis), on the circular frequency  $\omega$  of the applied external electric field. The curves  $a$ ,  $b$  and  $c$  correspond to the membrane conductivities of  $0.5 \times 10^{-5}$ ,  $1.0 \times 10^{-5}$ , and  $2.0 \times 10^{-5} \Omega^{-1}\text{m}^{-1}$ , respectively. Other parameters used in the calculation were  $r_0 = 10 \mu\text{m}$ ,  $\gamma = 0.9996$ ,  $k_c = 1.2 \times 10^{-19} \text{J}$ ,  $E_0 = 100 \text{V/cm}$ ,  $\sigma_w = 10^{-4} \Omega^{-1}\text{m}^{-1}$ ,  $\epsilon_w = 80\epsilon_0$ ,  $\epsilon_{\parallel} = 2\epsilon_0$ ,  $\Delta\epsilon = 6\epsilon_0$ .

for which  $\xi_{\infty} = 0$  holds can only be computed numerically. In figure 4, the transition boundary between prolate and oblate shape in the high frequency limit on the  $(\epsilon_{\parallel}/\epsilon_w, \Delta\epsilon/\epsilon_w)$  plane is plotted.

An insight into the high-frequency behaviour can also be obtained from the expanded expression (26). If in addition to the expansion in  $(1 - \gamma)$  an expansion in  $\epsilon_{\parallel}/\epsilon_w$  is employed (it is estimated  $\epsilon_{\parallel}/\epsilon_w \sim 1/40$ ), one obtains the following expression for the requirement for an oblate deformation in the high-frequency limit:

$$\Delta\epsilon \gtrsim 2\epsilon_{\parallel} . \quad (31)$$

It can also be seen that in the isotropic case ( $\Delta\epsilon = 0$ ), coefficient  $\xi_{\infty}$  attains the form (an expansion up to the first order in  $(1 - \gamma)$  is used):

$$\xi_{\infty} = \frac{4(\epsilon_w - \epsilon_{\parallel})^2}{9\epsilon_{\parallel}\epsilon_w} (1 - \gamma) , \quad (32)$$

which is always positive. Thus the deformation of a vesicle with isotropic membrane permittivity is always prolate in the high-frequency limit, which is consistent with the findings of Winterhalter and Helfrich [8].

*Low-frequency limit.* The condition for prolate deformation in the low-frequency limit is obtained from  $\lim_{\omega \rightarrow 0} s_2$ , yielding the criterion  $\xi_{\infty} + \xi_1 + \xi_2 = 0$  for the threshold between prolate and oblate shapes. Unlike the condition for the high-frequency limit, it depends on the dielectric permittivities as well as the conductivities of membrane and the aqueous medium. The sign of the exact expression  $\xi_{\infty} + \xi_1 + \xi_2$  depends on three parameters; here, they have been chosen to be  $\epsilon_{\parallel}/\epsilon_w$ ,  $\Delta\epsilon/\epsilon_w$ , and  $\sigma_m/\sigma_w$ . The comments on the dependence of the expression on  $\gamma$  in the high-frequency limit apply here as well.

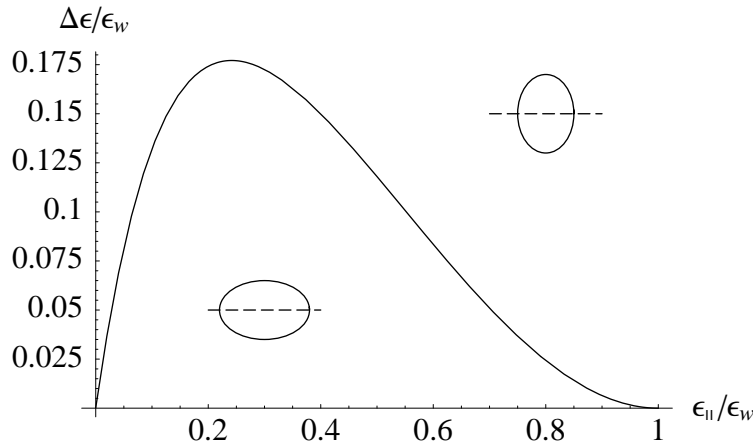


**Figure 4.** The boundary between the prolate and the oblate shape in the high-frequency limit as a function of the ratio between the permittivity of the membrane ( $\epsilon_{||}$ ) and the permittivity of the aqueous solution ( $\epsilon_w$ ). Deformation is oblate in the area above the curve and prolate in the area below the curve. For  $\epsilon_{||} \ll \epsilon_w$ , dependence can be approximated with a straight line  $\Delta\epsilon/\epsilon_w = 2\epsilon_{||}/\epsilon_w$ . The curve corresponds to a vesicle radius of 10  $\mu\text{m}$ , yielding  $\gamma = 0.9996$ .

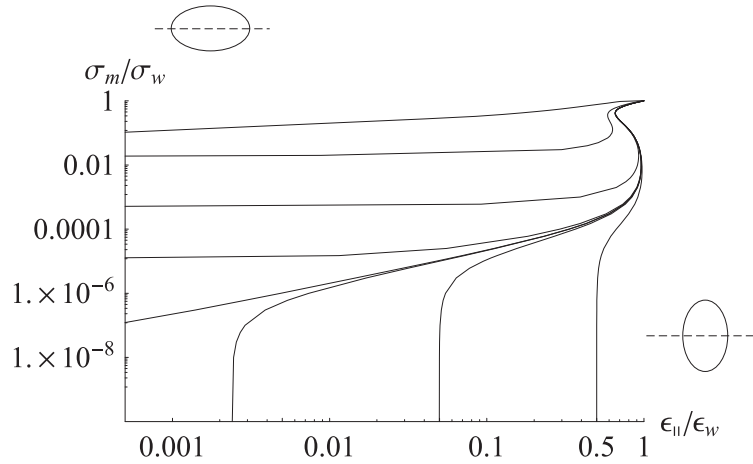


**Figure 5.** The boundary between the prolate and the oblate shape in the low-frequency limit as a function of the ratio between permittivity of the membrane  $\epsilon_{||}$  and permittivity of water  $\epsilon_w$  on the one hand and the ratio of membrane conductivity  $\sigma_m$  and the conductivity of the aqueous medium  $\sigma_w$  on the other hand. Deformation is prolate in the area above the curve valid for a particular value of dielectric anisotropy and oblate in the area below it. The delineation lines correspond to different values of dielectric anisotropy (from bottom to top):  $\Delta\epsilon = 0, 0.0144, 0.01592, 0.016, 0.018, 0.1, 3,$  and  $30 \epsilon_0$ . The curves are calculated for  $\gamma = 0.9996$ .

Its zero can only be computed numerically. In figure 5, the threshold between prolate and oblate shape in the low frequency on the  $(\epsilon_{||}/\epsilon_w, \sigma_m/\sigma_w)$  plane is plotted for several different values of  $\Delta\epsilon$ . The curves are plotted for  $\gamma = 0.9996$ , which corresponds to a vesicle radius of 10  $\mu\text{m}$ .

It is worth noting that for small values of anisotropy ( $\Delta\epsilon \approx 0$ ), curves intersect

the abscissa. For  $\Delta\epsilon = 0$ , the intersection point is approximately  $1/2 - (1 - \gamma)/3$ , meaning that for ratios  $\epsilon_{\parallel}/\epsilon_w$  lower than this value (this corresponds to all experimentally achievable cases), the deformation of a vesicle with a membrane of negligible conductivity in the low-frequency limit is prolate, while for the cases  $\epsilon_{\parallel}/\epsilon_w > 1/2 - (1 - \gamma)/3$ , the deformation in the low-frequency limit for the same vesicle is oblate. Increasing dielectric anisotropy lowers the threshold value, and at  $\Delta\epsilon/\epsilon_w \approx 0.0002$ , the deformation of a vesicle with a non-conductive membrane is always oblate in the low-frequency limit. This is consistent with the findings of Winterhalter and Helfrich [8], who have predicted prolate deformation in the low-frequency limit for a vesicle with no dielectric anisotropy and very small membrane conductivity  $\sigma_m/\sigma_w = 10^{-10}$ .

Again, additional insight can be obtained when one employs expansions in  $(1 - \gamma)$  and  $\epsilon_{\parallel}/\epsilon_w$ , yielding the following requirement for prolate deformation in the low-frequency limit:

$$\sigma_m > \frac{\sigma_w}{2} \left( \frac{\epsilon_{\parallel} - \epsilon_{\perp}}{\epsilon_w} - 2 \frac{\epsilon_{\parallel}\epsilon_{\perp}}{\epsilon_w^2} \right). \quad (33)$$

For  $\epsilon_{\perp} = 3\epsilon_{\parallel}$ , which also fulfills the requirement (31) obtained for oblate deformation in the high-frequency limit, (33) simplifies to

$$\sigma_m \gtrsim \frac{\epsilon_{\parallel}}{\epsilon_w} \sigma_w. \quad (34)$$

In (34), it has been taken into account that  $\epsilon_{\parallel}, \epsilon_{\perp} \ll \epsilon_w$ . Prolate deformation in the low-frequency limit for a vesicle with nonzero membrane anisotropy is only possible when the ratio of membrane conductivity and the conductivity of the aqueous solution exceeds the ratio of permittivities of membrane and the aqueous solution.

Another special case is the isotropic case ( $\epsilon_{\parallel} = \epsilon_{\perp} \ll \epsilon_w$ ). Here, the expression on the right-hand side (33) is negative, and so the inequality is always fulfilled, meaning that the deformation of a vesicle with no anisotropy in dielectric permittivity is always prolate in the low-frequency limit.

*Transition frequency.* It is also of interest to plot the transition frequency between the prolate and the oblate shape as a function of membrane conductivity. This corresponds to finding the zeroes of the following equation for different values of parameters:

$$\xi_{\infty} + \frac{\xi_1}{1 + \omega^2 \tau_1^2} + \frac{\xi_2}{1 + \omega^2 \tau_2^2} = 0. \quad (35)$$

Parameter space can be reduced by using a dimensionless frequency, as defined above. One can calculate the threshold dimensionless frequency numerically. Its dependence on the ratio between membrane conductivity and the conductivity of the aqueous medium ( $\sigma_m/\sigma_w$ ) for different values of dielectric anisotropy is plotted in figure 6. It can be seen that for values of  $\sigma_m/\sigma_w$  smaller than a certain threshold value – approximately given by (34) – one does not obtain a prolate-to-oblate transition at all.

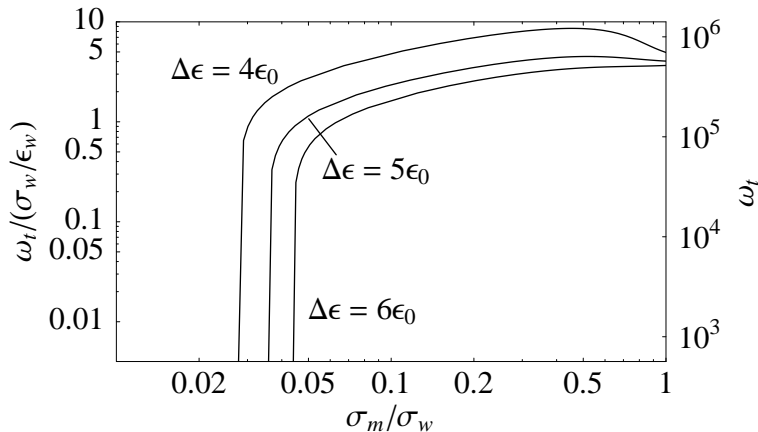


**Figure 6.** The dependence of the transition frequency between the prolate and the oblate shape on the value of the ratio between membrane conductivity and the conductivity of the aqueous medium ( $\sigma_m/\sigma_w$ ), plotted for three different values of dielectric anisotropy ( $\Delta\epsilon = 4, 5, 6 \epsilon_0$ ). The dependence is calculated for  $\epsilon_{\parallel} = 2\epsilon_0$ ,  $\gamma = 0.9996$ . On the left axis, the scale is plotted in terms of dimensionless frequency  $\omega_t/(\sigma_w/\epsilon_w)$ ; on the right axis, the scale is plotted in terms of circular frequency  $\omega_t$  for  $\sigma_w = 10^{-4} \Omega^{-1}\text{m}^{-1}$  and  $\epsilon_w = 80\epsilon_0$ .

#### 4. Discussion

The treatment presented in this paper largely follows the outline by Winterhalter and Helfrich [8]. It is important to note, however, that substituting isotropic values for the coefficients  $\xi_{\infty}$ ,  $\xi_1$ ,  $\xi_2$ ,  $\tau_1$  and  $\tau_2$  into expression (25) *does not* lead to the same result as equation (21) in their article. The expansions in factors  $\beta$  and  $\gamma$  used by Winterhalter and Helfrich show non-analytical behaviour, where consecutive expansions in  $\gamma$  and  $\beta$  yield a result different from the one obtained by consecutive expansions conducted in the opposite order, i.e., an expansion in  $\beta$ , followed by an expansion in  $\gamma$ . Using Winterhalter and Helfrich's values of material constants, one can see that  $\beta > \gamma$  holds in the high-frequency limit, while in the low-frequency limit  $\beta < \gamma$  holds. Due to this, the frequency dependence of the simplified expression they obtained by series expansion differs qualitatively from the exact expression from which the simplified expression was derived – while the deformation described by the exact expression decreases with the increasing frequency, the simplified expression increases. In this paper, we avoided using series expansion in  $\beta$  altogether, expressing it explicitly with the frequency  $\omega$  and the material constants independent of frequency. The expression (25) may provide a better approximation to the exact expression than the one used by Winterhalter and Helfrich, as it retains the frequency dependence of the exact expression, while the expansion they used employs an expansion in  $\beta$  and is thus actually limited to the low-frequency range only.

In the previous section, we have developed criteria within the framework of our model, under which the vesicle shape is prolate in the low-frequency limit and oblate in

the high-frequency limit. The criteria we obtained however opened a couple of questions about their physical relevance: the tangential component of permittivity is predicted to exceed its normal component threefold, the membrane conductivity is predicted to be higher than the earlier estimates [8].

- (i) *Membrane permittivity.* Within the framework of the presented model, a criterion for an oblate shape in the high-frequency limit was obtained, requiring that the tangential component of the dielectric permittivity tensor of the phospholipid membrane exceeds its radial component by approximately threefold:  $\epsilon_{\perp} \gtrsim 3\epsilon_{\parallel}$ . This is in qualitative agreement with an abundance of experimental evidence claiming that the zwitterionic phosphatidylcholine headgroup is oriented almost parallel to the surface of a hydrated bilayer and its movement is essentially confined to a plane normal to the membrane, employing techniques such as X-ray diffraction, neutron diffraction,  $^2\text{H}$  nuclear magnetic resonance (NMR) and  $^{31}\text{P}$  NMR as well as molecular simulation studies (see [24] and the references therein).
- (ii) *Membrane conductivity.* Another criterion was obtained for a prolate vesicle shape in the low-frequency limit, which required that the ratio of membrane conductivity and conductivity exceeds the ratio of membrane permittivity and the permittivity of the aqueous medium. In practice, this means a relatively high value for membrane conductivity:  $\sigma_m \sim 10^{-5} \text{ S m}^{-1}$ . This exceeds not only the value for a thin layer of oil,  $\sigma_m \sim 10^{-14} \text{ S m}^{-1}$  [8], but also some other estimates for membrane conductivity ( $\sigma_m \sim 10^{-7} \text{ S m}^{-1}$ ) [11]. The high value of conductivity could be attributed to the impurities in the lipid and the transient submicroscopic pores in the membrane (step 1 in the accepted five-step description of electropermeabilization, [25]). A simple model treating the intact membrane and the pores as resistors connected in parallel shows that the total area of pores must account for approximately 1/1000 of the total membrane area, which corresponds to 1000 pores with an area of  $100 \text{ \AA}^2$  per  $1 \text{ \mu m}^2$  of membrane area. This significantly –  $10^6$ – $10^8 \times$  – exceeds the density of spontaneous pore formation in the membrane [26]. This latter value increases, however, with an the applied electric field [27], even though the electric field strength in our setup is approximately 70–300 $\times$  lower than its threshold value necessary for the pore expansion into micrometer-sized “macropores” [28]. An initial membrane tension present in a vesicle with a relative volume very close to 1 (the estimate for the vesicle shown in figure 1 is  $v = 0.9993 \pm 0.0007$ ) also works in the same direction. Altogether, a high value of membrane conductivity predicted by the presented model remains a poorly understood effect, and awaits further investigations before a definitive conclusion can be made.

*Geometry considerations.* It has been our intention to build the simplest possible model which would explain the observed frequency-dependent prolate-to-oblate shape transition for small deformations and yield a clear physical picture of the phenomenon. The validity of the model decreases once we depart from small deformation. A possible

extension of the model lies in a more appropriate description of the vesicle geometry, i.e. spheroidal instead of spherical. An effort in the suggested direction might benefit from the treatment of a spheroid vesicle with a permeable membrane [29], as well as from the calculations of transmembrane voltage for the case of zero membrane conductance [30, 31] and the solution for the electric potential for the general anisotropic case [13].

## 5. Conclusions

The proposed model provides a theoretical explanation for the observed prolate-to-oblate transition of phospholipid vesicle shape, when the frequency of the applied AC electric field increases, in the case when the electrical properties of the aqueous solution inside the vesicle do not differ from the properties of the aqueous solution outside the vesicle. Vesicle deformation at varying frequency was calculated numerically. Using an expansion into Taylor series we also derived a simplified expression for the deformation. The expression retains the frequency dependence of the exact expression and may provide a better substitute for the expression that Winterhalter and Helfrich obtained by series expansion, which was found to be valid only in the limit of low frequencies. The model with the anisotropic membrane permittivity imposes two constraints on the values of material constants: tangential component of dielectric permittivity tensor of the phospholipid membrane must exceed its radial component by approximately a factor of 3; and membrane conductivity has to be relatively high, approximately one tenth of the conductivity of the external aqueous medium. Both constraints seem to be justified to a certain degree by the claims found in the literature.

## Acknowledgments

This work has been supported by the Slovenian Research Agency research grant P1-0055.

## References

- [1] Zimmermann U and Neil G A, eds 1996 *Electromanipulation of Cells* (Boca Raton: CRC Press) ISBN 0-8493-4476-X
- [2] Jones T B 1995 *Electromechanics of particles* (Cambridge, New York, Melbourne: Cambridge University Press) ISBN 0-561-43196-4
- [3] Foster K R and Schwan H P 1996 in C Polk and E Postow, eds, *Handbook of biological effects of electromagnetic fields* (Boca Raton, New York, London, Tokyo: CRC Press) pp 25–102 2nd ed ISBN 0-8493-0641-8
- [4] Schwan H P 1957 *Adv. Biol. Med. Phys.* **5** 147–209
- [5] Helfrich W 1973 *Z. Naturforsch. C* **28** 693–703
- [6] Helfrich W 1974 *Z. Naturforsch. C* **29** 182–183
- [7] Harbich W and Helfrich W 1979 *Z. Naturforsch. A* **34** 1063–1065
- [8] Winterhalter M and Helfrich W 1988 *J. Coll. Int. Sci.* **122** 583–586
- [9] Mitov M D, Méléard P, Winterhalter M, Angelova M I and Bothorel P 1993 *Phys. Rev. E* **48** 628–631
- [10] Peterlin P, Sevšek F, Svetina S and Žekš B 1993 *Acta Pharmaceut.* **43** 143–145



- [11] Sukhorukov V L, Meedt G, Kürscher M and Zimmerman U 2001 *J. Electrostat.* **50** 191–204
- [12] Ko Y T C, Huang J P and Yu K W 2004 *J. Phys.: Condens. Matter* **16** 499–509
- [13] Ambjörnsson T and Mukhopadhyay G 2003 *J. Phys. A: Math. Gen.* **36** 10651–10665
- [14] Ambjörnsson T, Apell S P and Mukhopadhyay G 2004 *Phys. Rev. E* **69** 031914–1–031914–8
- [15] Simeonova M and Gimsa J 2005 *J. Phys.: Condens. Matter* **17** 7817–7831
- [16] Hyuga H, Kinoshita Jr K and Wakabayashi N 1991 *Jpn. J. Appl. Phys.* **30** 2649–2656
- [17] Hyuga H, Kinoshita Jr K and Wakabayashi N 1993 *Bioelectrochem. Bioenerg.* **32** 15–25
- [18] Aranda S, Riske K A, Lipowsky R and Dimova R 2006 *Biophys. J.* **90** 503A
- [19] Dimova R, Aranda S, Bezlyepkina N, Nikolov V, Riske K A and Lipowsky R 2006 *J. Phys.: Condens. Matter* **18** S1151–S1176
- [20] Peterlin P, Svetina S and Žekš B 2000 *Pflügers Arch. Eur. J. Physiol.* **439** R139–R140
- [21] Kummrow M and Helfrich W 1991 *Phys. Rev. A* **44** 8356–8360
- [22] Niggemann G, Kummrow M and Helfrich W 1995 *J. Phys. II France* **5** 413–425
- [23] Landau L D, Lifshitz E M and Pitaevskiĭ L P 1984 *Electrodynamics of Continuous Media* 2nd ed vol 8 of *Course of Theoretical Physics* (Oxford: Butterworth-Heinemann) ISBN 0-7506-2634-8
- [24] Raudino A, Castelli F, Brigante G and Carnetti C 2001 *J. Chem. Phys.* **115**(17) 8238–8250
- [25] Teissie J, Golzio M and Rols M P 2005 *Biochim. Biophys. Acta* **1724** 270–280
- [26] Raphael R M, Waugh R E, Svetina S and Žekš B 2001 *Phys. Rev. E* **64** 051913
- [27] Neu J C and Krassowska W 1999 *Phys. Rev. E* **59**(3) 3471–3482
- [28] Riske K A and Dimova R 2005 *Biophys. J.* **88** 1143–1155
- [29] Sokirko A V, Pastushenko V P, Svetina S and Žekš B 1994 *Bioelectrochem. Bioenerg.* **34** 101–107
- [30] Kotnik T and Miklavčič D 2000 *Biophys. J.* **79** 670–679
- [31] Gimsa J and Wachner D 2001 *Biophys. J.* **81** 1888–1896